International Journal of Engineering and Geosciences
https://dergipark.org.tr/en/pub/ijeg
e-ISSN 2548-0960

Human micro-doppler detection and classification studies at Mersin University using real outdoor experiments via C-band FMCW radar

Onur Tekir [*1], **Caner Özdemir** [1]

[1] *Mersin University, Department of Electrical-Electronics Engineering, Türkiye, onur_tek@hotmail.com, cozdemir@mersin.edu.tr*

Cite this study: Tekir, O., & Özdemir, C. (2024). Human micro-doppler detection and classification studies at Mersin University using real outdoor experiments via C-band FMCW radar. International Journal of Engineering and Geosciences, 9 (2), 211-220

https://doi.org/10.26833/ijeg.1380658

Keywords
Micro-doppler radar
Radar imaging
Spectrogram
Human detection and classification

Research Article

Received: 24.10.2023
Revised: 21.01.2024
Accepted: 24.01.2024
Published:23.07.2024

Abstract

In this work, a unique radar hardware is introduced for human-gait micro-Doppler studies. The developed radar sensor operates in C-band microwave frequencies. We share several outdoor experiments at Mersin University facilities to detect and characterize human walking and running movements. In these experiments, various walking and running movements were performed with different people. To examine the Doppler properties of human motion, raw data gathered is transformed onto 2D joint-time-frequency plane. The generation of micro-Doppler signatures in the transformed data is the first step in the extraction of features of the walking/running human motion. It is shown that the directions, durations, range distances as well as torso and limb velocities of walking and running human movements in each experiment are successfully obtained from these micro-Doppler signatures.

1. Introduction

Human detection and motion classification offer many advantages for applications such as search and rescue, intelligent environments, and security. Infrared, lidar [1-3], acoustic, vibration/seismic, and visual sensors have long been used in human recognition and detection systems. Radar technology, on the other hand, offers advantages in human detection applications because it can detect at longer distances, is more comprehensive and can operate in all weather conditions [4-7].

With today's developments, the need for long-range radar systems that can detect targets with low radar cross-sectional area [8] such as humans is increasing significantly. In the last ten years, many studies have been published on the automatic classification of various human movements and different targets from radar signals [9]. In human classification studies, the radar signature of a human being is usually very different from the radar signature of other targets.

If the signal sent by the radar hits a target that is moving relative to the radar, the frequency of the return signal from the target is slightly different from the frequency of the transmitted signal. This phenomenon is called "Doppler shift" [10]. The amplitude of the Doppler shift depends on the speed of the target relative to the radar and the frequency of the transmitted signal. If the target has parts that oscillate, vibrate, and rotate in addition to the translational motion, additional modulations due to these parts are observed in the return signal in addition to the basic Doppler shift. This phenomenon is called the micro-Doppler effect and the signal returned from the target is called the micro-Doppler signature of the target [11].

Micro-Doppler has been utilized for target recognition in many studies, especially in applications such as pedestrian safety with automotive radar networks [12-13]. In 2010, Van Dorp and Groen conducted a basic classification study on human arm swing using Frequency-Modulated Continuous-Wave (FMCW) radar networks with micro-Doppler analysis [14].

In any surveillance application, real-time estimation and visualization of human posture is critical for threat analysis. Human movement and gait characteristics (hand, arm and leg movements) can be detected by applying detailed radar signal techniques on micro-

Doppler echoes. In addition to the radar image of holistic human body motion, micro-Doppler features contain unique spectral information about gait characteristics. Mainly because the legs, arms and wrists do not move at constant speed, the micro-Doppler effect exhibits a periodic characteristic. Time-varying micro-Doppler features due to different parts of the body are deduced by combined time-frequency analyses [15]. Time-frequency micro-Doppler images describe the motion characteristics. The characteristics of human gait have been studied in detail by researchers in the fields of biomechanics and computer vision [16-18]. However, the use of radar signals in this field is quite recent [19]. Geisheimer experimentally demonstrated that a human spectrogram can be obtained from signals reflected from different parts of the body [20]. In this paper, we present recent experiments that we have conducted at Mersin University in characterization and analysis of the human movements including basic walking and running activities.

Organization of paper is as follows: In the second section, the micro-Doppler radar sensor that we have developed and the data gathering arrangement are introduced. In the third next section, various experiments the micro-Doppler experiments and corresponding micro-Doppler images based on spectrogram are presented together with numerical analysis after the evaluation of the constructed micro-Doppler images. The final section summarizes and concludes the work presented in this paper.

2. Method

2.1. Radar sensor

A micro-Doppler radar hardware has been developed which is based on a frequency modulated continuous wave (FMCW) transceiver [Ancortek's SDR-KIT-580AD]. Figure 1a shows the block diagram of our radar sensor. Two two-by-three microstrip patch antenna array with an antenna gain of more than 12 dBi for the whole frequency bandwidth of 400 MHz at the center frequency of 5800 MHz. Figure 1b depicts the perspective view of the developed radar device in which the locations of the transmitting and receiving antennas are labelled. For the experiments, the chirp time interval is chosen to be 1 ms such that it can cover the extremum values of full human micro-Doppler signatures for indoor and outdoor activities. More precisely, the radar can measure Doppler frequencies from -500 Hz to + 500 Hz. Radar device has the power output of approximately 0.08 watts. The FMCW transceiver equipment is controlled by the on-board PC board. The Matlab script, including the implementation of all signal processing routines, was used together with the on-board PC hardware. A 7-inch LCD touchscreen display is integrated for the easy use of the operator. A power board was used to provide +5V to all the hardware of the micro-Doppler radar sensor module [21]. The front and back photos of this radar sensor are shown in Figure 1c, where all electronic components can be viewed.

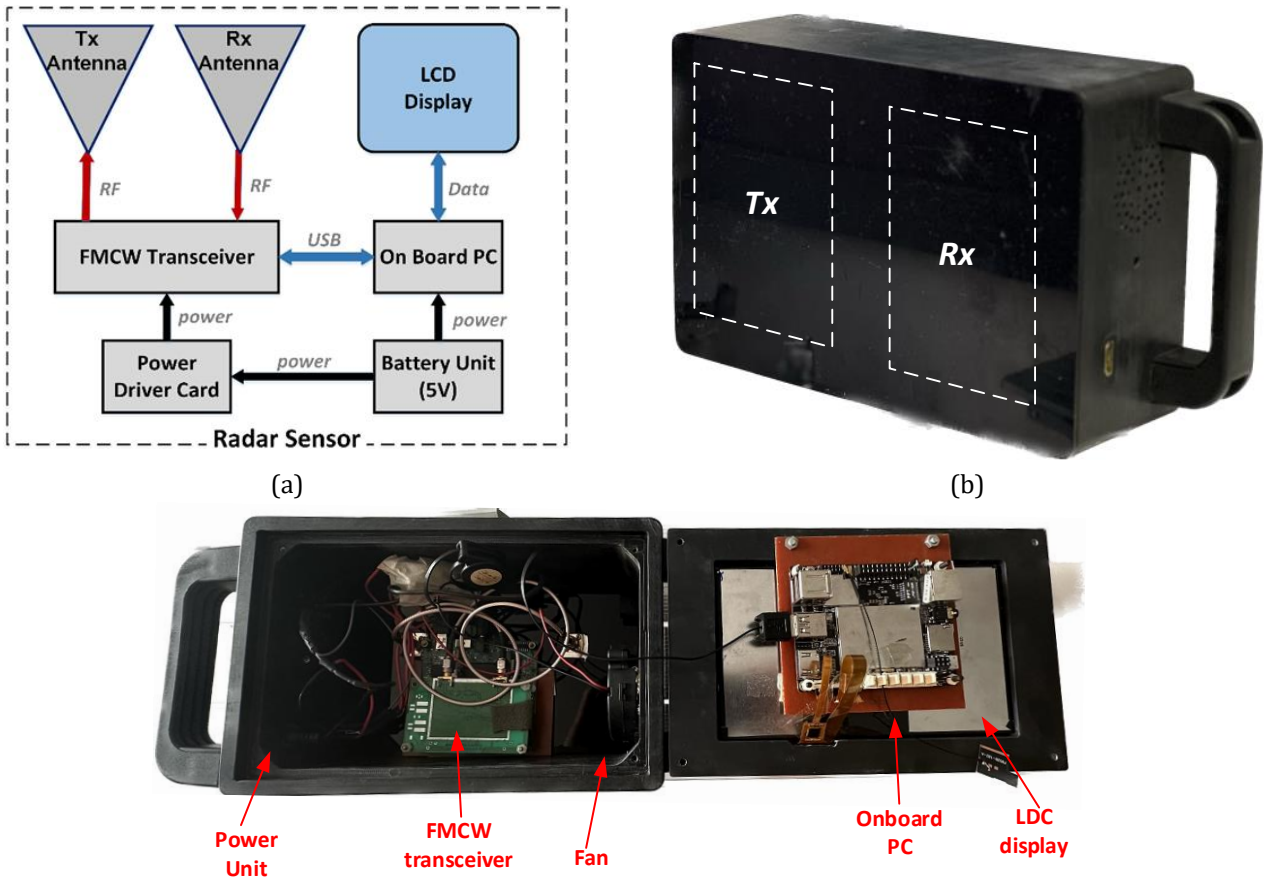

Figure 1. Prototyped micro-Doppler radar sensor: (a) block diagram, (b) Perspective view, (c) inner hardware.

2.2. Experimental set-up

This radar sensor was used for experimental research to detect human movement and possibly classify human body parts. In the experimental setup, the radar sensor was placed on a tripod at a height of 1m above the ground level and various people walked, walked away and/or ran towards the radar sensor. Figure 2a, 3a, 4a, 5a and 6a show some photos from the experimental scenes.

3. Results and discussion

Five different experiments were accomplished for several types of human movements: In the first experiment, the human walked towards and then moved from the radar at approximately 26 m range distance with swinging both arms as shown in Figure 2a, maintaining a relatively stationary velocity during the data collection period of 35 s. The micro-Doppler signature was then generated by applying a short-time Fourier transform (STFT) process, i.e. spectrogram, to the FMCW-based time-domain scattered electric field data; $E^s(t)$ obtained the micro-Doppler signature as (Equation 1).

$$E^s(\tau, f) = \int_{-\infty}^{\infty} E^S(t) \cdot w(t-\tau) exp(-j2\pi f t) dt \qquad (1)$$

Here w(t) is a 200-point Hamming-type sliding window corresponding to 0.2 seconds with 95% overlap [10]. A notch filter [22] was also applied to minimize the effect of static clutter around the DC frequencies and to highlight the true signature. After these operations, obtained micro-Doppler signature image was extracted as shown in Figure 2b. As can be seen from the image, both the main motion of the torso and the swinging arm signatures can be easily recognized. The Doppler frequency of the torso starts from f_D = 0Hz (for a fixed human target) at t = 0 and reaches a maximum value of about 65 Hz (corresponding to a speed of 6.05 km/h) just after t = 7s as seen from the time-Doppler image in Figure 2b. Figure 2c shows the time-velocity image, which allows the velocity information to be detected more easily during the movement time.

In the second experiment, the man walked towards and then moved away from the radar with still arms at about 28 m along the range distance, keeping a relatively stable speed during the 35 s data collection period as shown in Figure 3a. The Doppler frequency of the torso starts at f_D = 0Hz (for a fixed human target) at t = 0 and reaches a maximum value of about 63 Hz (corresponding to a torso speed of 5.86 km/h) just after t = 7s, as seen from the time-Doppler image in Figure 3b. Figure 3c shows the time-velocity image, which allows the velocity information to be detected more easily during the movement time.

In the third experiment the man walked towards to the radar from approximately 8.5 m at range distance again for a time duration of 8 s as pictured in Figure 4a. After using the identical spectrogram examination described above, a micro-Doppler spectrogram image was extracted as shown in Figure 4b. If this image is carefully examined, one can undoubtedly observe that the man has no movement at t = 0 and moves away from the radar as time progresses, reaching an average body Doppler frequency of about 38 Hz (equivalent to torso speed of 3.58 km/s). Once more, the signatures of the swinging arms and the responses of other body pieces are distinctly noticeable in Figure 4b. Figure 4c shows the time-velocity image, which allows the velocity information to be detected more easily during the movement time.

In the fourth experiment, the human first ran towards the radar, then away from the radar and finally towards the radar, sustaining a reasonably stable velocity during the 18 s data acquisition period. Each running lap has approximately 21 m. An image from the experiment and the Doppler spectrogram are shown in Figure 5a and Figure 5b, respectively. From the spectrogram in Figure 5b, it is clearly read that the Doppler frequency can reach a highest value of about 210 Hz, equivalent to a running velocity of 19.55 km/h. This amount, evidently, includes the sum of both torso and arm/hand velocities. When computing the speed of the torso, the average Doppler frequency of the torso was measured to be 135 Hz when the man was running towards the radar at a uniform speed. Hence, this Doppler frequency amount specifies a nominal torso velocity measurement of 12.57 km/h. Figure 5c shows the time-velocity image, which allows the velocity information to be detected more easily during the movement time.

For the fifth experimentation, two men have run in an outdoor field as portrayed in Figure 6a. First, one man run towards to radar at the same time other man run away from the radar by preserving a uniform velocity during the data gathering interval of 7 s. Each man has run up to a maximum distance of around 22 m along the range. It is obviously interpreted from the spectrogram in Figure 6b that the first running man's Doppler frequency can attain a highest value of approximately 226 Hz which matches to a running velocity of 21.04 km/h. The second running man's Doppler frequency can achieve a largest amount of around 261 Hz which resembles a running speed of 24.3 km/h. These values; obviously, contain the sum of the speeds of torso, arms, and hands. The torso average Doppler frequencies of running men were measured to be 150 Hz and 155 Hz, respectively during men were running towards the radar with a uniform velocity. So, these men's Doppler frequency values provide a nominal torso speed measurement of 13.96 km/h and 14.43 km/h, respectively. Figure 6c shows the time-velocity image, which allows the velocity information to be detected more easily during the movement time. The flow diagram in Figure 7 shows how to obtain the characteristics of the movement by using the information on the spectrogram obtained by using the short-time Fourier transform.

4. Conclusion

In this paper, we have presented a radar sensor that we have specially developed for the detection and classification of human micro-Doppler characteristics. As shared in the second and third sections, several

experiments were conducted outdoors using. We have demonstrated throughout experiments that the radar sensor has the capability of detecting human motions such as walking and running with good fidelity. By utilizing the time-frequency tool of spectrogram [23], it is possible to further analyze the micro-Doppler features of these motions including, characterization such as walking with still arms or running and calculation of other distinct features such as velocity information of human motion and range distance of the man, etc. Such extracted features are very crucial and thus, can be used for many useful applications in detecting and classifying men, women, children, and possibly different animals.

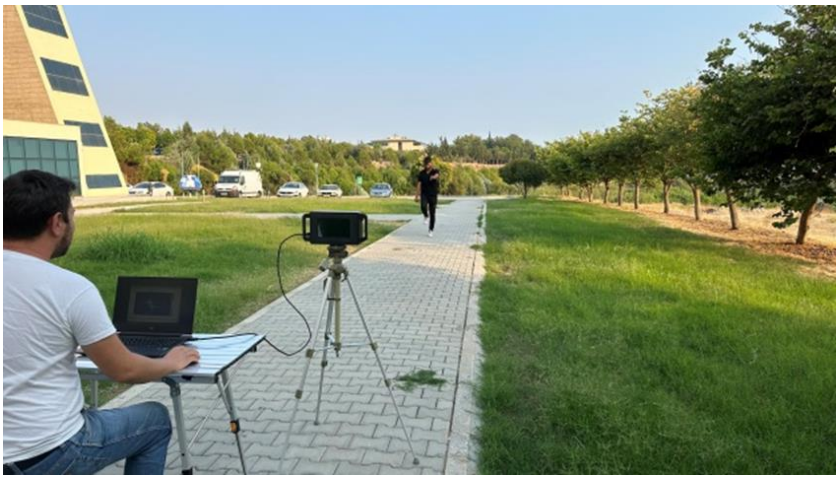

(a)

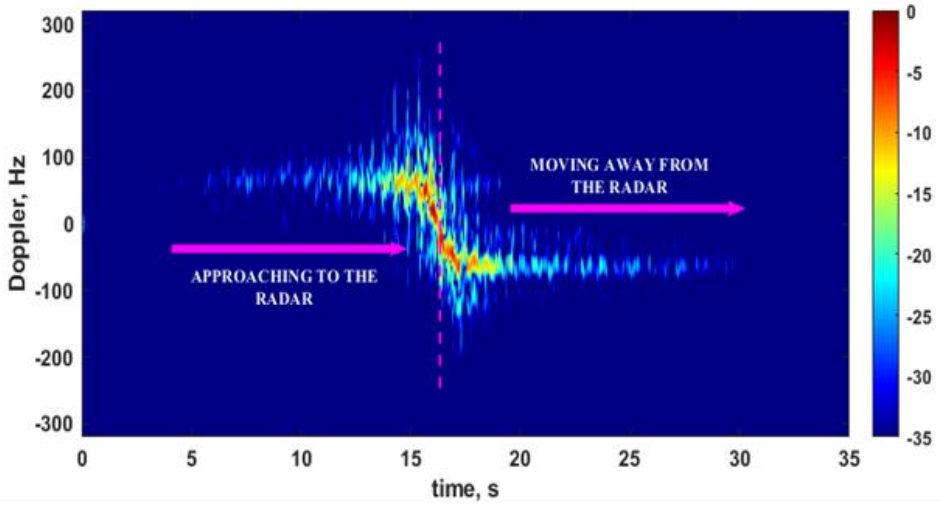

(b)

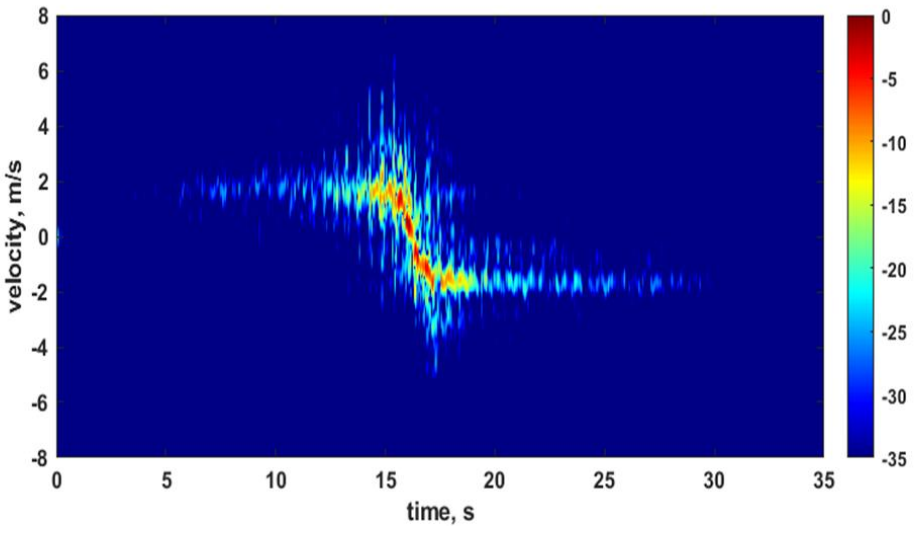

(c)

Figure 2. (a) The man first approached the radar and then moved away radar while walking with swinging arms, (b) corresponding spectrogram image (c) spectrogram image with velocity information.

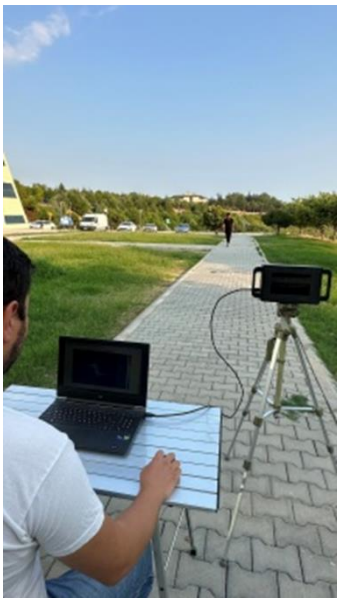

(a)

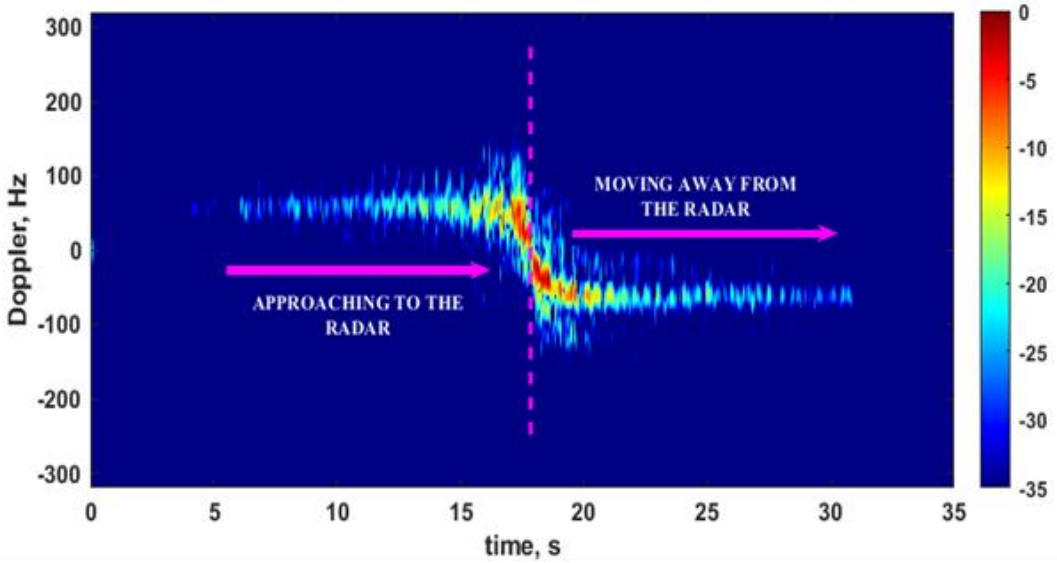

(b)

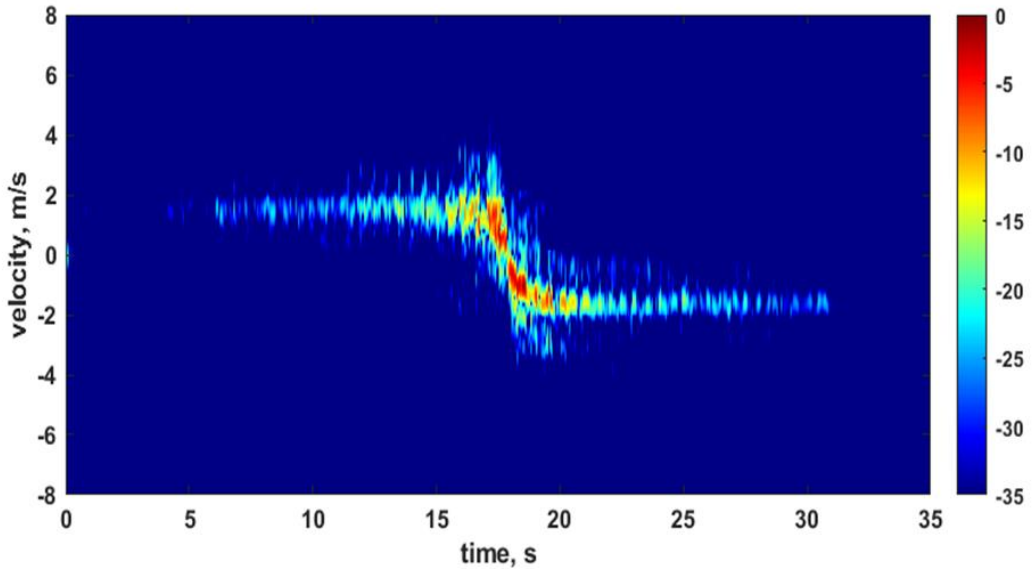

(c)

Figure 3. (a) The man approached the radar and then moved away from the radar while walking with still arms, (b) corresponding spectrogram image (c) radar image on time-velocity plane.

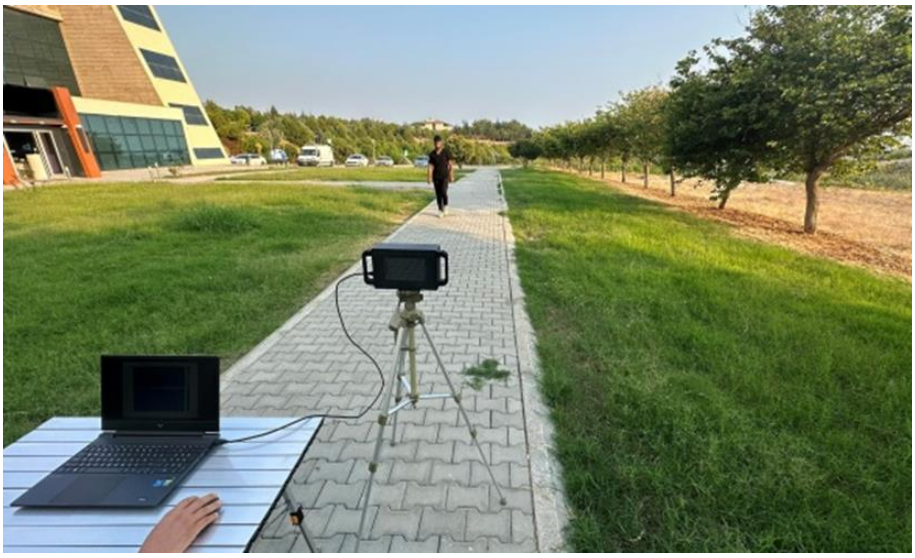

(a)

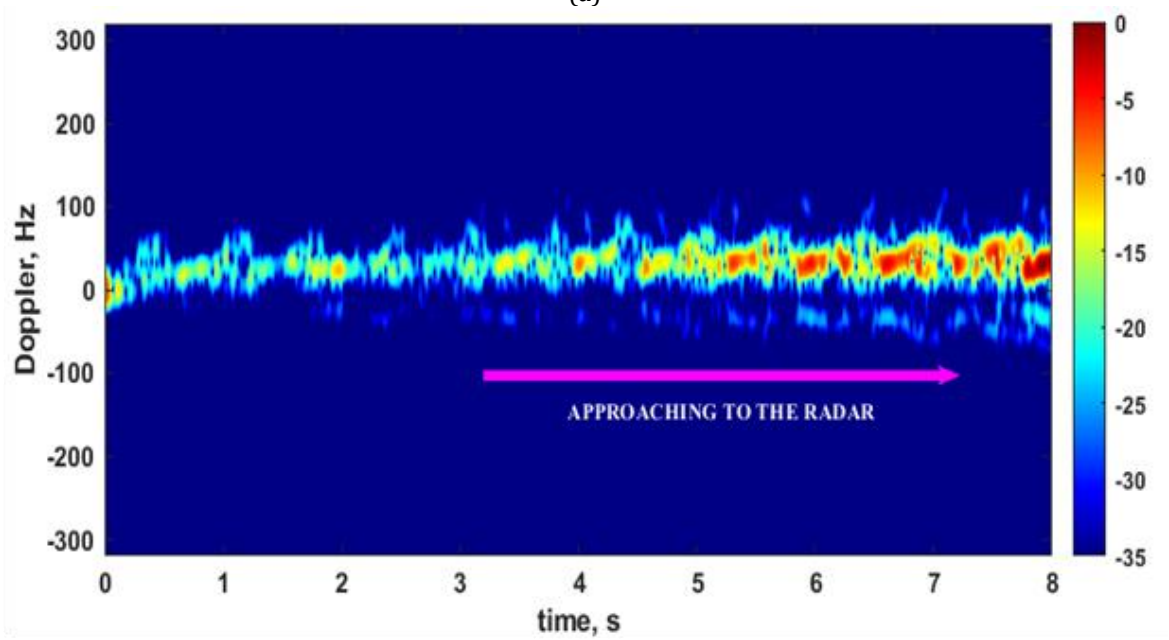

(b)

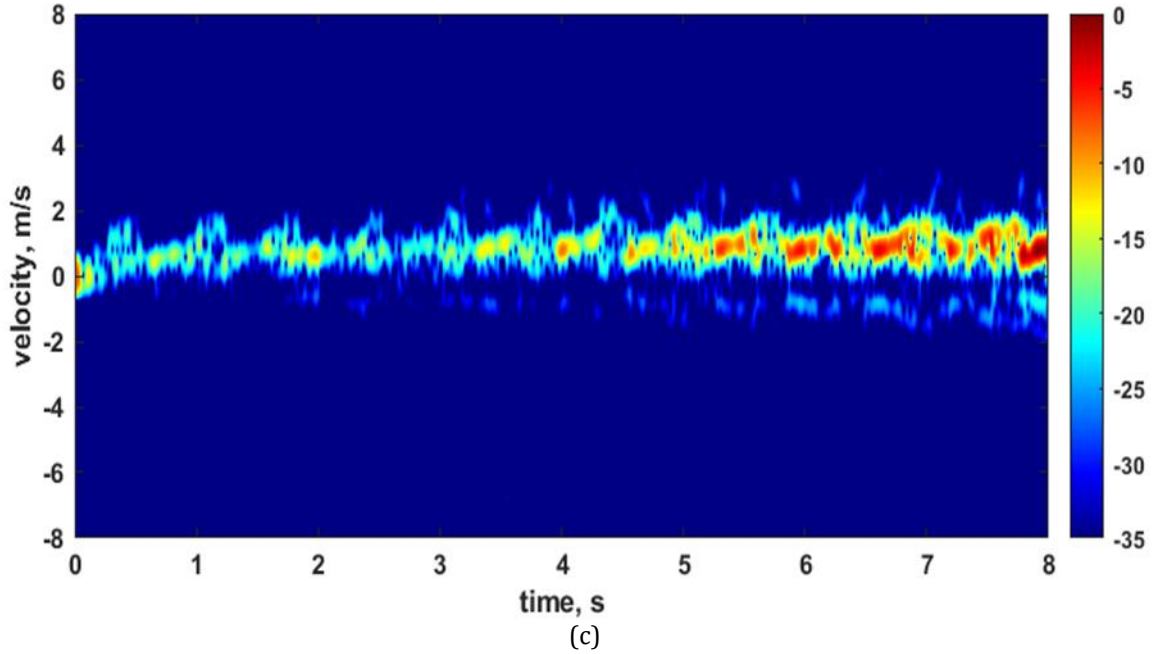

(c)

Figure 4. (a) The man approached the radar while walking with still arms, (b) corresponding spectrogram image (c) radar image on time-velocity plane.

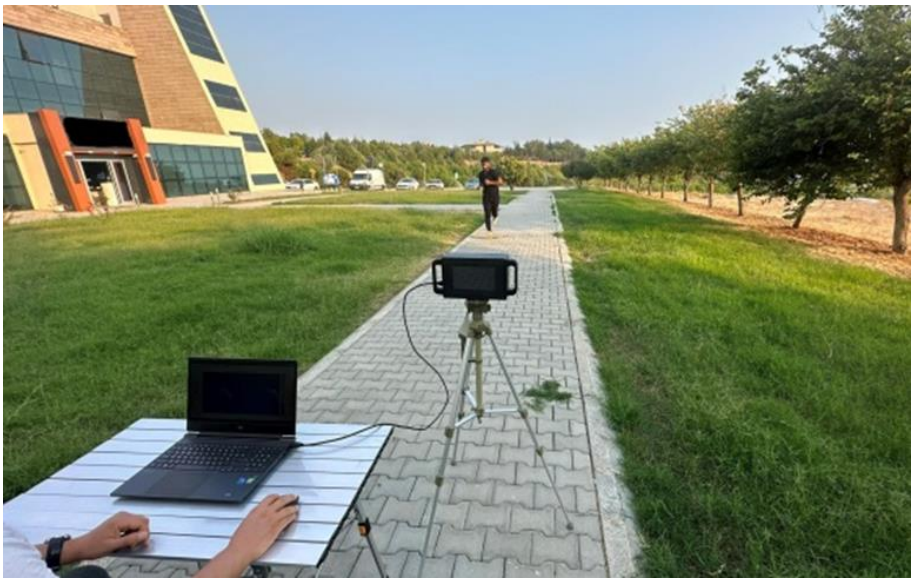

(a)

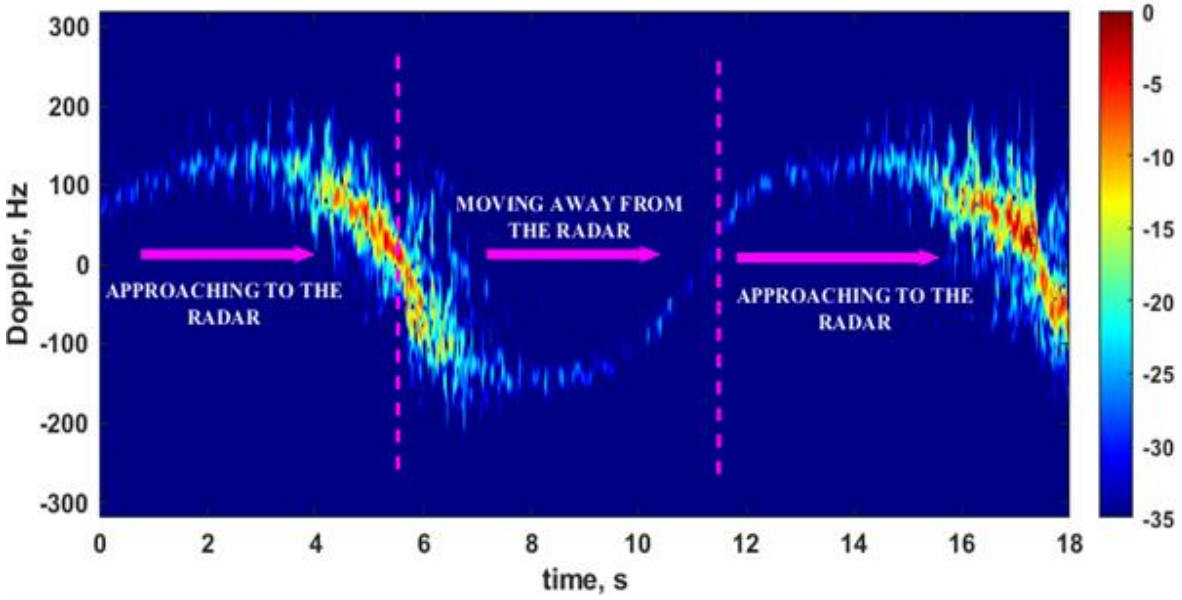

(b)

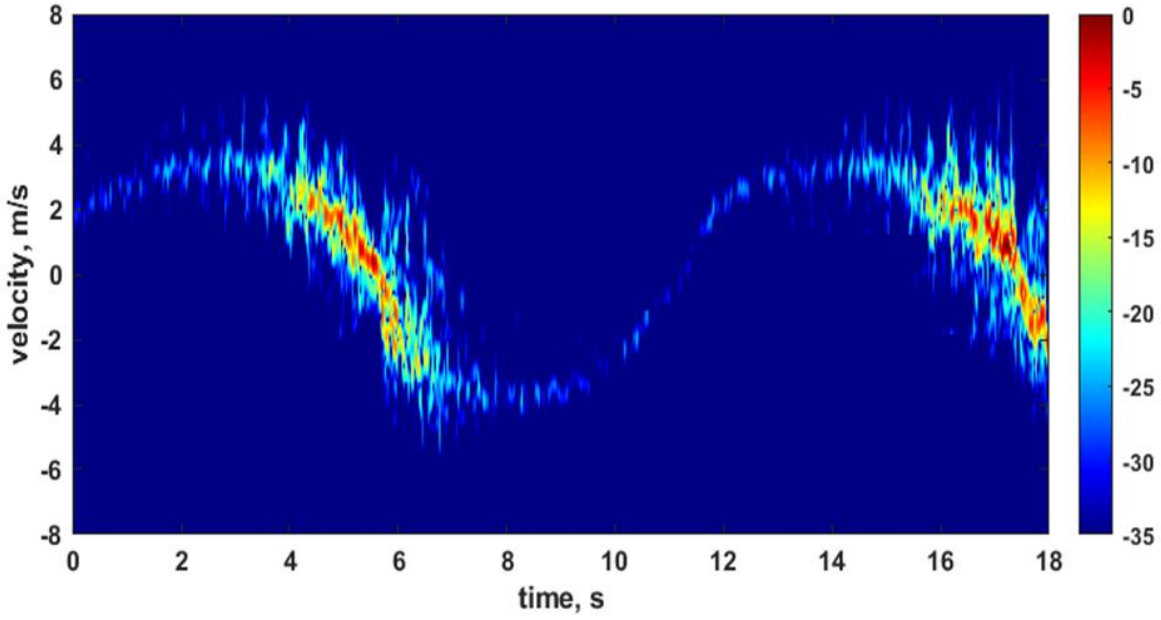

(c)

Figure 5. Running experiment: (a) The man first approached to the radar, then moved away from the radar, and finally approached the radar again, (b) corresponding spectrogram image (c) radar image on time-velocity plane.

(a)

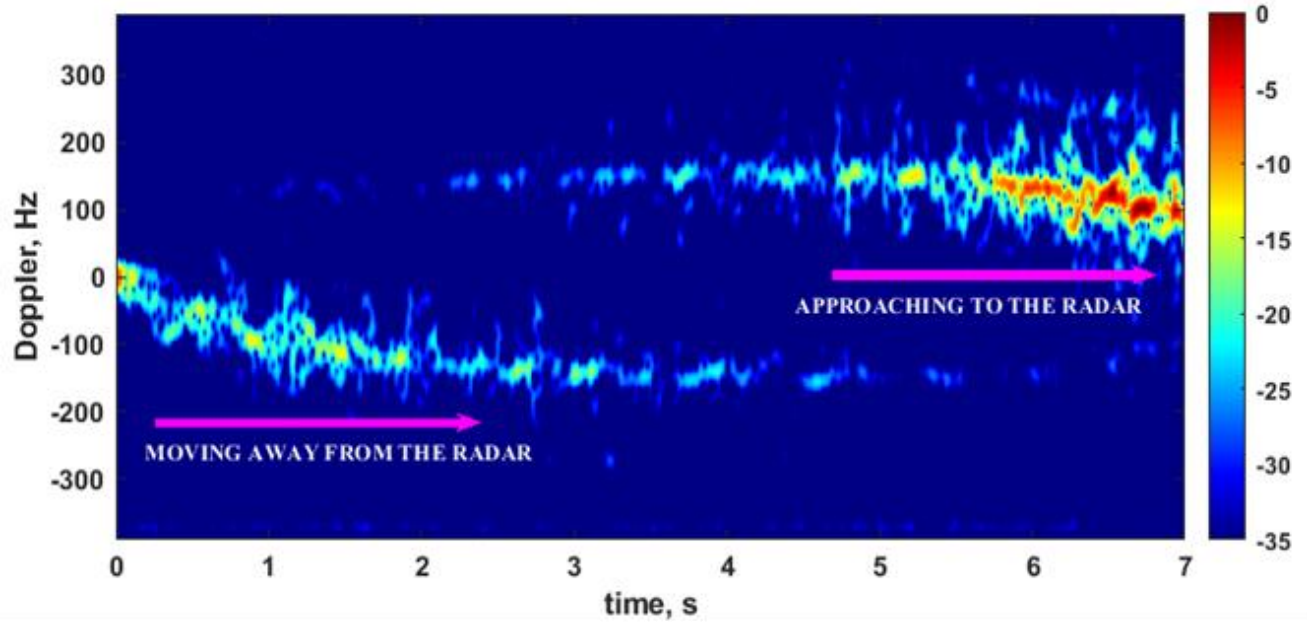

(b)

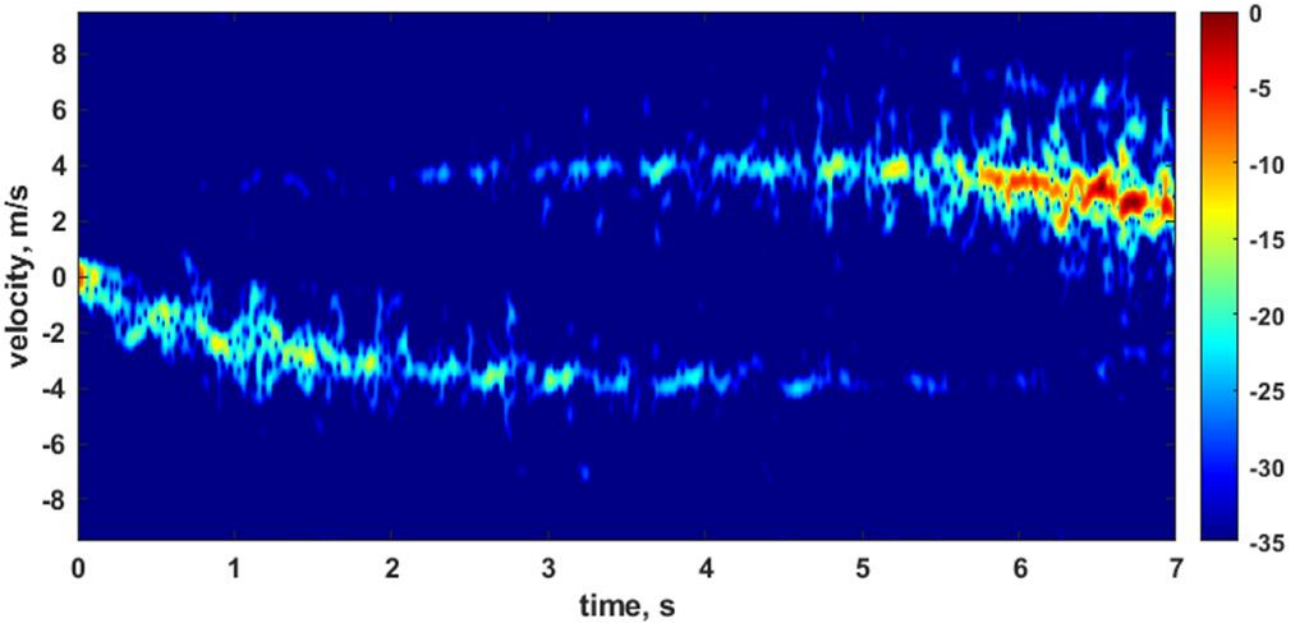

(c)

Figure 6. Two running men experiment (a) The men run opposite directions, (b) corresponding spectrogram image (c) spectrogram image with velocity information.

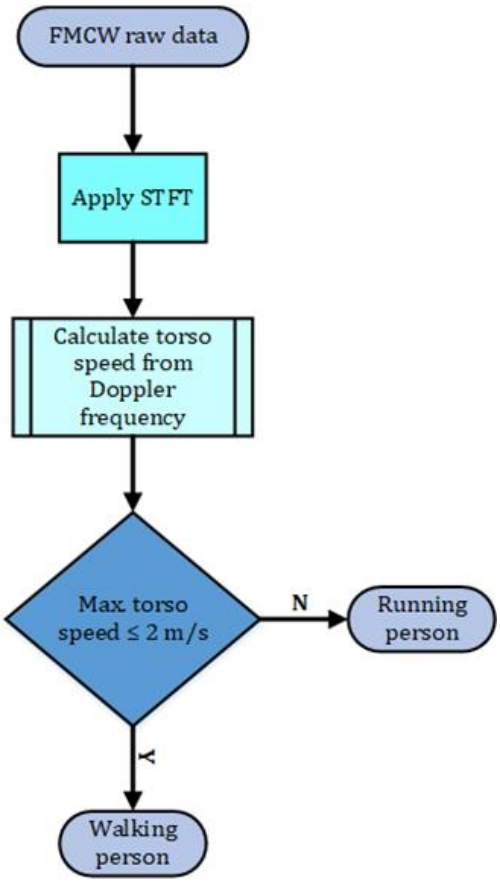

Figure 7. Classification of the movements according to the Doppler frequency with a flow diagram.

Acknowledgement

This work is supported by Mersin University Scientific Research Unit under Project No. 2018-2-TP3-2924. Authors would like to thank Mr. Gökhan Karabacak, Mr. Ahmet Özbek and Mrs. Yurdagül Olgun for their help during experiments.

Author contributions

Onur Tekir: Investigation, data curation, methodology, software, field study, writing-original draft preparation
Caner Özdemir: Conceptualization, validation, writing, reviewing, and editing.

Conflicts of interest

The authors declare no conflicts of interest.

References

1. Ağca, M. (2020). PALS, ICESat/GLAS ve ICESat-2 lazer sistemleri ve kullanım alanları. Geomatik, 5(1), 27-35. https://doi.org/10.29128/geomatik.560344
2. Navruz, M. (2017). Airborne LİDAR Ve Dted2 verilerinde yükseklik (H) karşılaştırması. Geomatik, 2(3), 112-117. https://doi.org/10.29128/geomatik.319270
3. Sevgen, S. C., & Karsli, F. (2020). Automatic ground extraction for urban areas from airborne lidar data. Turkish Journal of Engineering, 4(3), 113-122. https://doi.org/10.31127/tuje.641501
4. Yılmaz, B., & Özdemir, C. (2017). Design and prototype of a compact, ultra wide band double ridged horn antenna for behind obstacle radar applications. Turkish Journal of Engineering, 1(2), 76-81. https://doi.org/10.31127/tuje.316696
5. Demirci, Ş., & Özdemir, C. (2021). An investigation of the performances of polarimetric target decompositions using GB-SAR imaging. International Journal of Engineering and Geosciences, 6(1), 9-19. https://doi.org/10.26833/ijeg.665175
6. Demirci, Ş., & Özdemir, C. (2020). Anechoic chamber measurements for circular isar imaging at Mersin University's Meatrc Lab. International Journal of Engineering and Geosciences, 5(3), 150-159. https://doi.org/10.26833/ijeg.649961
7. Akgül, M. A. (2018). Sentetik açıklıklı radar verilerinin taşkın çalışmalarında kullanılması: Berdan Ovası Taşkını. Geomatik, 3(2), 154-162. https://doi.org/10.29128/geomatik.378123
8. Özdemir, C. (2020). Radar cross section analysis of unmanned aerial vehicles using predics. International Journal of Engineering and Geosciences, 5(3), 144-149. https://doi.org/10.26833/ijeg.648847
9. Gurbuz, S. Z., Melvin, W. L., & Williams, D. B. (2011). A nonlinear-phase model-based human detector for radar. IEEE Transactions on Aerospace and Electronic Systems, 47(4), 2502-2513. https://doi.org/10.1109/TAES.2011.6034647
10. Ozdemir, C. (2021). Inverse synthetic aperture radar imaging with MATLAB algorithms. John Wiley & Sons.
11. Chen, V. C. (2019). The micro-Doppler effect in radar. Artech house.

12. Kim, Y., & Ling, H. (2009). Human activity classification based on micro-Doppler signatures using a support vector machine. IEEE Transactions on Geoscience and Remote Sensing, 47(5), 1328-1337. https://doi.org/10.1109/TGRS.2009.2012849
13. Heuel, S., & Rohling, H. (2012, May). Pedestrian classification in automotive radar systems. 13th International Radar Symposium, 39-44. https://doi.org/10.1109/IRS.2012.6233285
14. van Dorp, P., & Groen, F. C. (2010). Human motion estimation with multiple frequency modulated continuous wave radars. IET Radar, Sonar & Navigation, 4(3), 348-361. https://doi.org/10.1049/iet-rsn.2009.0015
15. Chen, V. C., & Ling, H. (2002). Time-frequency transforms for radar imaging and signal analysis. Artech house.
16. Hurmuzlu, Y., Basdogan, C., & Carollo, J. J. (1994). Presenting joint kinematics of human locomotion using phase plane portraits and Poincaré maps. Journal of Biomechanics, 27(12), 1495-1499. https://doi.org/10.1016/0021-9290(94)90199-6
17. Boulic, R., Thalmann, N. M., & Thalmann, D. (1990). A global human walking model with real-time kinematic personification. The Visual Computer, 6, 344-358. https://doi.org/10.1007/BF01901021
18. Boulic, R., Ulicny, B., & Thalmann, D. (2004). Versatile walk engine. Journal of Game Development, 1(1), 29-50.
19. Chen, V. C. (2000). Analysis of radar micro-Doppler with time-frequency transform. In Proceedings of the Tenth IEEE Workshop on Statistical Signal and Array Processing (Cat. No. 00TH8496), 463-466. https://doi.org/10.1109/SSAP.2000.870167
20. Geisheimer, J. L., Greneker III, E. F., & Marshall, W. S. (2002). High-resolution Doppler model of the human gait. In Radar Sensor Technology and Data Visualization, 4744, 8-18. https://doi.org/10.1117/12.488286
21. Tekir, O., Yılmaz, B., & Özdemir, C. (2023). Signal preprocessing routines for the detection and classification of human micro-Doppler radar signatures. Microwave and Optical Technology Letters, 65(8), 2132-2149. https://doi.org/10.1002/mop.33684
22. Persico, A. R., Clemente, C., Gaglione, D., Ilioudis, C. V., Cao, J., Pallotta, L., ... & Soraghan, J. J. (2017). On model, algorithms, and experiment for micro-Doppler-based recognition of ballistic targets. IEEE Transactions on Aerospace and Electronic Systems, 53(3), 1088-1108. https://doi.org/10.1109/TAES.2017.2665258
23. Ozdemir, C., & Ling, H. (1997). Joint time-frequency interpretation of scattering phenomenology in dielectric-coated wires. IEEE Transactions on Antennas and Propagation, 45(8), 1259-1264. https://doi.org/10.1109/8.611245